ISSN1027-5495. Functional Materials, 31, No.3 (2024), p. 351-358
doi:http://dx.doi.org/10.15407/fm31.03.351

Composite material based on zirconium dioxide partially stabilised with cerium oxide and aluminium oxide for bioengineering applications

***E.S.Hevorkian*[1,2,3], *O.M.Morozova*[2], *V.P.Nerubatskyi*[2], *V.O.Chyshkala*[1], *D.S.Sofronov*[4], *S.Moya*[5], *A.Abarrategi*[5,6], *B.Arnaiz*[5], *M.A.Bondarenko*[7], *R.V.Vovk*[1,2]**

[1]V.N.Karazin Kharkiv National University, 4 Svobody Sq., 61022 Kharkiv, Ukraine
[2]Ukrainian State University of Railway Transport, 7 Feierbakh Sq., 61050 Kharkiv, Ukraine
[3]University of Life Sciences in Lublin, 13 Akademicka, 20-950 Lublin, Poland
[4]SSI "Institute for Single Crystals" NAS of Ukraine, "Institute for Single Crystals" NAS of Ukraine 60 Nauky ave., 61072 Kharkiv, Ukraine
[5]CIC biomaGUNE, 182, Paseo Miramón, Donostia, 20014 San Sebastián, Spain
[6]IKERBASQUE, Basque Foundation for Science, 5 Plaza Euskadi, 48009 Bilbao, Spain
[7]Kharkiv National Medical University, 4 Nauky ave., 61022 Kharkiv, Ukraine

Received February 16, 2024

The work presents the results of research of compacted ceramic systems based on zirconium dioxide partially stabilized with cerium oxide and aluminium oxide, with additives of silicon carbide and silica; these materials could potentially be used as surgical implants or devices. The composite materials ZrO_2–5wt.%CeO_2–10wt.%SiC have shown higher biocompatibility with the human osteosarcoma cell line MG-63 than samples of compositions Al_2O_3–20wt.%SiO_2–10wt.%ZrO_2 and ZrO_2–5wt.%CeO_2. Samples demonstrated hydrophilic behavior according to contact angle measurements. Zeta potential experiments showed that the nanoparticles were negatively charged in all cases in this study. Since the samples compacted in the temperature range of 1300–1600°C are biocompatible with MG-63 cells, zirconia-based ceramics compacted at temperatures higher 1300°C may improve implant osseointegration as a result of further research.

Keywords: cell viability, composite, electroconsolidation, implants, zirconium dioxide.

Композитний матеріал на основі діоксиду цирконію, частково стабілізованого оксидом церію та оксидом алюмінію, для біоінженерних застосувань. *Е.С.Геворкян, О.М.Морозова, В.П.Нерубацький, В.О.Чишкала, Д.С.Софронов, S.Moya, A.Abarrategi, B.Arnaiz, М.А.Бондаренко, Р.В.Вовк*

У роботі наведено результати дослідження компактних керамічних систем діоксиду цирконію, частково стабілізованого оксидом церію та оксидом алюмінію, з добавками

карбіду кремнію та кремнезему як матеріалів для потенційного застосування як хірургічних імплантатів або пристроїв. Встановлено, що композитні матеріали складу ZrO_2–5мас.%CeO_2–10мас.%SiC мають вищу біосумісність із клітинною лінією остеосаркоми людини MG-63, ніж зразки складу Al_2O_3–20мас.%SiO_2–10мас.%ZrO_2 та ZrO_2–5мас.%CeO_2. Зразки продемонстрували гідрофільну поведінку згідно з вимірюванням контактного кута. Експеримент з дзета-потенціалом показав, що наночастинки були негативно заряджені в усіх випадках цього дослідження. Оскільки зразки, пресовані в діапазоні температур 1300–1600°C, є біосумісними з клітинами MG-63, кераміка на основі цирконію, спресована при високих температурах 1300°C, могла б посилити остеоінтеграцію імплантату в подальших дослідженнях.

1. Introduction

Ceramics based on zirconium dioxide are a perspective material for various applications. The development of ZrO_2–CeO_2–SiC composites is promising and requires research in order to develop ceramic systems with optimum composition.

Due to their increased resistance to environmental influences and high transformation temperatures, zirconia based ceramic systems form a new class of shape memory ceramic materials [1]. Fibrous highly porous ceramics of the CeO_2–ZrO_2–Y_2O composition are used in thermochemical cycles [2], demonstrating improved gas exchange and high rates of renewal.

Formation of high-density CeO_2–SiC composite ceramics by electrospark plasma sintering has been reported [3]. The authors report that the introduction of up to 20 mol% of α-SiC particles causes a shift in the temperature dependences and shrinkage rate towards higher heating temperatures with a simultaneous decrease in the maximum shrinkage values and the powder shrinkage rate. However, the uneven sintering of the studied ceramics requires the use of submicron α-SiC particles.

Since the selection of an optimal system composition determines the final product properties, the authors [4] synthesized CeO_2–ZrO_2 and ZrO_2–CeO_2/SiO_2 systems as fuel cell components. It was found that the compositions of tetragonal and cubic phases are ZrO_2–15wt.%CeO_2 and CeO_2–5wt.%ZrO_2 respectively.

Three-component ceramic systems are in the focus of attention since they allow increasing the strength of ceramic systems without changing their structure due to simultaneous doping with two cations. Thus, in work [5] a composition of the tetragonal modification Al_2O_3–SiO_2–ZrO_2 was synthesized. The systems of 5wt.%Al_2O_3–80wt.%ZrO_2–12wt.%CeO_2 and 50wt.%Al_2O_3–88wt.%ZrO_2–12wt.%CeO_2 were synthesized in [6]; its main crystalline phase is a solid solution based on tetragonal zirconium dioxide. Studies of the system 10wt.%Sc_2O_3–1wt.% CeO_2–89wt.% ZrO_2 [7] have shown that the blocks 10S1CeSZ have a cubic phase structure at room temperature after sintering.

Doping with cerium oxide leads to improvement of electric characteristics of the materials [8]: Y_2O_3–ZrO_2–CeO_2 solutions exhibit satisfactory ionic conductive properties at elevated temperatures and mixed type at a high temperature and low oxygen pressure; at the same time, CeO_2 activity values in CeO_2–Y_2O_3 and CeO_2–Y_2O_3–ZrO_2 systems are characterized by negative deviations from ideal values. The authors [9] investigated the electrical properties of the Y_2O_3–ZrO_2–CeO_2 system and found the conductivity of the system to be ~1.10 eV.

In [10], a self-repair of ceramic composite material with the composition Y_2O_3–ZrB_2–SiC–ZrC–ZrO_2 was obtained and investigated. It was established that the zirconium dioxide content in ceramics leads to an increase in the oxide layer thickness on the sample surface and an increase in the sample mass due to occurrence of oxidation processes on the ceramics surface. Self-repair of the ceramic composite material of the composition ZrB_2–SiC–ZrC–ZrO_2 was obtained and investigated in [10]. It is established that the zirconium dioxide content in ceramics leads to an increase in the oxide layer thickness on the sample surface and the increased sample mass due to oxidation processes on ceramics surface.

The three-component ceramic systems can be synthesized by different methods: the compositions MoO_3–CeO_2–ZrO_2, WO_3–CeO_2–ZrO_2 [11] and the ceramic system TiO_2–CeO_2–ZrO_2 [12] were produced by the sol-gel method, and Al_2O_3–ZrO_2–Ce_2O – by simultaneous deposition of all components [13].

The method of nanopowder synthesis by decomposition from fluoride salts has been successfully applied to manufacture composite materials for various applications: Al_2O_3–SiC nanocomposite material for the manufacture of cutting inserts [14], composite material ZrO_2–3wt.% Y_2O_3 for constructional application [15]

and one of Al_2O_3–15wt.% AlN composition for instrumental application [16].

Composite materials can be obtained by various methods: ceramics of $SiC–Al_2O_3/Yb_2O_3$ composition was formed by spark plasma sintering and showed a flexural strength of 720 MPa and crack resistance of 4 $MPa·m^{1/2}$ [17]; the system of ZrO_2–20wt.% Y_2O_3 was obtained by hot vacuum pressing with 99% relative density and microstructure of 270 nm [18]. The choice of the sintering mode is an important task in obtaining nanoscale ceramic systems, since the prevention of grain growth during heat treatment and the principle of structure inheritance at all forming stages ensure the production of functional ceramics [19].

Due to the combination of high mechanical characteristics and aesthetic qualities, ceramic systems based on Al_2O_3, ZrO_2, and $ZrO_2–Al_2O_3$ are widely used in biomedicine. For example, zirconia ceramics have found orthopedic use as hip and knee prostheses, temporary supports for hip heads, tibial plates and dental crowns [20]. Since zirconia-based ceramics are nontoxic, noncarcinogenic, hypoallergenic, noninflammatory, biocompatible, biofunctional, aesthetically pleasing, corrosion resistant, and heat resistant materials, it can replace titanium as a material for dental implants [21]. The bioinert behavior and wettability of ceramics, in addition to their mechanical properties, allow these systems to be implemented in tissue engineering.

This paper investigates ceramic systems based on partially stabilized zirconia, which were formed by hot pressing of nanopowders obtained by decomposition from fluoride salts, as well as the biocompatibility of the developed systems.

2. Experimental

Hydrofluoric acid HF, concentrated nitric acid HNO_3, an aqueous ammonia solution NHO_4OH, zirconium metal, and polyvinyl alcohol (PVC) from Reahim have been used. Distilled water has been used for preparation of the solutions. Zirconium dioxide particles were obtained as follows: zirconium metal weighing 4 g was placed in a 100 mL Teflon beaker; 10 mL of hydrofluoric acid and 10 mL distilled water were added. Then, 60 ml of distilled water and the calculated amount of polyvinyl alcohol were added to the resulting solution with constant stirring. The resulting mixture was stirred for 1 hour and then 20 ml of aqueous ammonia solution was added and stirred for 30 minutes. The precipitation process was carried out at 20, 50 and 80°C. The mass content of polyvinyl alcohol in the ratio m(Zr): m(PVC) varied as 1:0.1, 1:0.5 and 1:1.

Upon completion, the resulting precipitate was filtered off, washed with distilled water and dried at room temperature for 48 hours. The dried precipitate was then heated in a muffle furnace to 800°C (heating rate 100°C/hour) for 4 hours, and then the resulting zirconium dioxide was cooled to room temperature.

The surface morphology of the obtained powders was studied using a JSM-6390LV scanning microscope (SEM). Ceramic samples were formed by hot vacuum pressing via electroconsolidation [22, 23].

The wettability was assessed using a DSA100 Drop shape analyzer by a sessile drop method at room temperature using distilled water and a drop volume of 2μ (n=3). Wettability values were evaluated with the supplied software (ADVANCE V.1.7.2.1, Krüss, Hamburg, Germany). To determine the angle of contact with water, the method of optimal approximation of an ellipse was used in accordance with the curvature of the drop shape. Zeta potential was measured using a Malvern Zetasizer at 25 °C. Data were processed with ZS XPLORER software.

Four discs of different compositions were sintered by the electroconsolidation method: ZrO_2–5wt.% CeO_2–10wt.%SiC, ZrO_2–5wt.% CeO_2 at 1300 °C, holding time is 3 min; ZrO_2–5wt.% CeO_2 at 1300°C, holding time is 3 min; ZrO_2–5wt.% CeO_2 at 1400°C, holding time is 3 min; Al_2O_3–20wt.% SiO_2–10wt.% ZrO_2 at 1600°C, holding time is 5 min. They were cut into 4 equal size pieces (Tecnalia Spain). Three of them were employed as triplicates for biological assays and one of them was used for physicochemical characterization. They were sterilized twice for 15 minutes in 70% ethanol, three times for 5 minutes in sterile PBS, and for 5 minutes in sterile water, and finally they were sterilized with UV radiation for 30 minutes on both sides.

40,000 MG-63 cells (CRL-1427, ATCC, human osteosarcoma cell line) were seeded on each piece of discs or the polystyrene well bottom as control and left to adhere for 4 h at 37°C and 5wt.% CeO_2. Then, 500 μl warm media was added and cultured at 37°C and 5wt.% CeO_2 for 28 days. The cells cultured in Dubelcco´s Modified Eagle Medium (DMEM) media (61965-026, Gibco, UK) were supplemented before being

used with 10% fetal bovine serum (10500-064, Gibco, UK), 2 mML – glutamine (25030024, Gibco, UK), and 50 U/ml penicillin and 50 μg/ml streptomycin (15070063, Gibco, UK).

The cell tracker red CMTPX (Thermofisher) C34552 at the concentration of 10μM in warm complete DMEM new medium was used to replace the cell medium and incubated for 30 min at 37°C and 5wt.% CeO_2. After incubation, the medium was removed, and cells were washed twice with warm complete DMEM medium. Before imaging, all the pieces were turn upside-down using sterile tweezers. Both the MG-63 cells on the scaffolds and at the bottom of the plastic well were imaged with the 1sm880 Zeiss confocal microscope using the Plan-Apochromat 10x/0/45M27 objective. The live fluorescent cells were excited with the 561 nm-laser and detected with a short bandpass at 620–650 nm to minimize the introduction of autofluorescence from the material into this channel. The material pieces were imaged in another channel in reflection mode using the405 nm-laser and detected at 380–430 nm. Next, to test for calcium deposition, the cell-containing materials were turned upside-down and washed three times with warmed complete medium, being carefully not to disturb the MG-63 cell monolayer, then fixed with 10% formalin for 30 min under a fume hood and washed three times with tap water. Then, they were stained with alizarin red solution (Merck, TMS-008) for 20 min at room temperature, washed with tap water for 5 min three times and left to dry overnight. The pieces of materials were transferred to a 12 well plate and imaged in a straight Leica stereomicroscope with 5x magnification. The images were acquired with a Leica color camera controlled by the Leica LAS suite software. Since alizarin red is also fluorescent, to obtain fluorescent images of cells in an inverted microscope, each of the piece were turned upside down and 1 ml of PBS containing 5mg/ml 2-[4-(aminoiminomethyl)phehyl]-1H-Indole-6-carboximidamide hydrochloride(DAPI)(D9542, Sigma Aldrich,USA) was added to every well containing MG-63 cells on the materials. The images were taken with the lsm880 Zeiss confocal microscope using the Plan-Apochromat 10x/0.45 M27 objective. To visualize calcium deposits stained with alizarin red, excitation at 514 nm and emission in the range of 540–675 nm were used; Dapi-stained nuclei were visualized using excitation at 405 nm and emission at 430–500 nm; material was visualized using excitation at 405 nm and emission at 400–420 nm. The Zen Blue software was employed for image analysis.

Comparative studies included alizarin red staining of calcium deposits 28 days after seeding. Images were obtained with a Leica stereomicroscope (pink) and a confocal Zeiss microscope (red). Cell Tracker Red staining was performed to examine cell density and morphology 24 days after seeding. Images were obtained using the confocal Zeiss microscope and represented in green. Control cells were seeded on plastic wells (polystirene). Scale bar equals 50 μm.

On day 28 post-seeding, the cell viability was quantified by colorimetry of the resulting product after 4h incubation of the cells at 37°C and 5wt.%CeO_2 with warm complete medium containing 1/10 Deep Blue Cell Viability reagent (Biolegend, 424701). Then, 100μl of supernanant was transferred to triplicate wells of a 96-well plate with a black transparent bottom and the fluorescence was measured in a plate spectrophotometer (Tecan, geniosPro) at excitation/emission wavelengths of 535/590 nm. The results were normalized to the measurements of the control sample (cells growing at the bottom of the plastic/polystyrene well).

The data were processed using SPSS Statistics 17.0 (SPSS Inc., USA). The number of values in each group was n=13. The normality of the distribution of the compared parameters was checked by the Kolmogorov-Smirnov criterion. The main statistical characteristics (sample mean, standard deviation) were determined; the reliable probability for which the reliable interval was constructed was 0.95. The paired two-sample Student's t-test was used to determine the statistical significance of the difference between two sample means in samples with normal distribution. All the results obtained were significant (p<0.01 in all comparison groups).

3. Result and discussion

Mixtures of initial nanopowders were annealed at 800°C with a holding time of 60 min. The images of nanopowders (Fig. 1) show different structure of nanopowders with average size of particles about 10 μm. Sample ZrO_2–5wt.%CeO_2 has an uniform rounded shape with smooth and homogeneous particles. ZrO_2–5wt.% CeO_2–10wt.%SiC powder has angular-shape particles with a rough and non-uniform surface. Al_2O_3–20wt.% SiO_2–10wt.% ZrO_2 is a powder with fibrous particles and a uniform

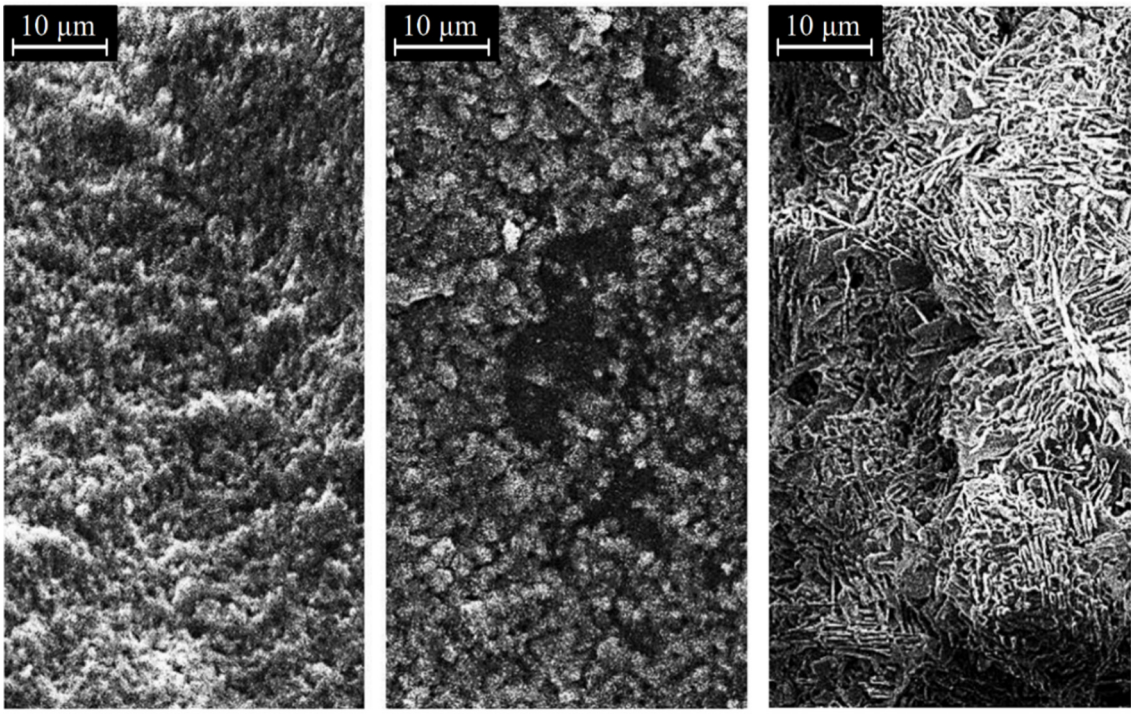

Fig. 1. Microphotographs of ZrO_2–5wt.% CeO_2 (a), ZrO_2–5wt.% CeO_2–10wt.%SiC (b), Al_2O_3–20wt.% SiO_2–10wt.% ZrO_2 (c) of particles, annealed at 800°C, holding time – 60 min

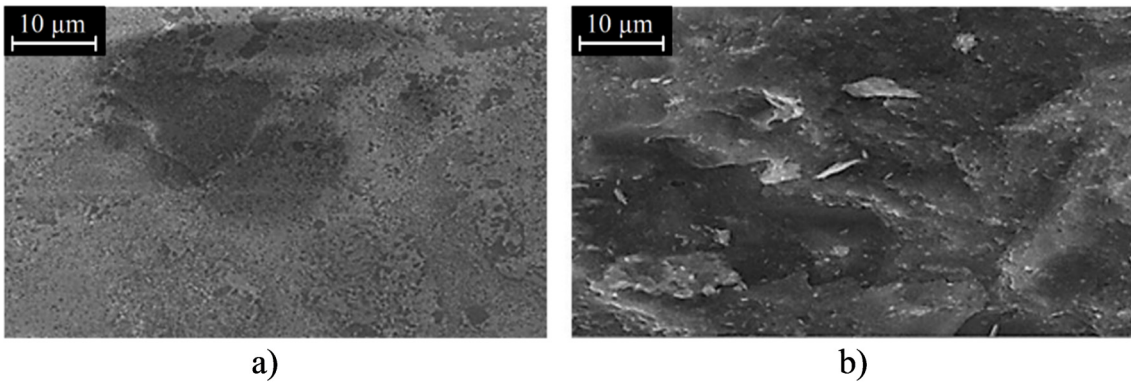

Fig. 2. Microphotographs of ceramic composition samples ZrO_2–5wt.% CeO_2–10wt.% SiC (a) and Al_2O_3–20wt.% SiO_2–10wt.% ZrO_2 (b)

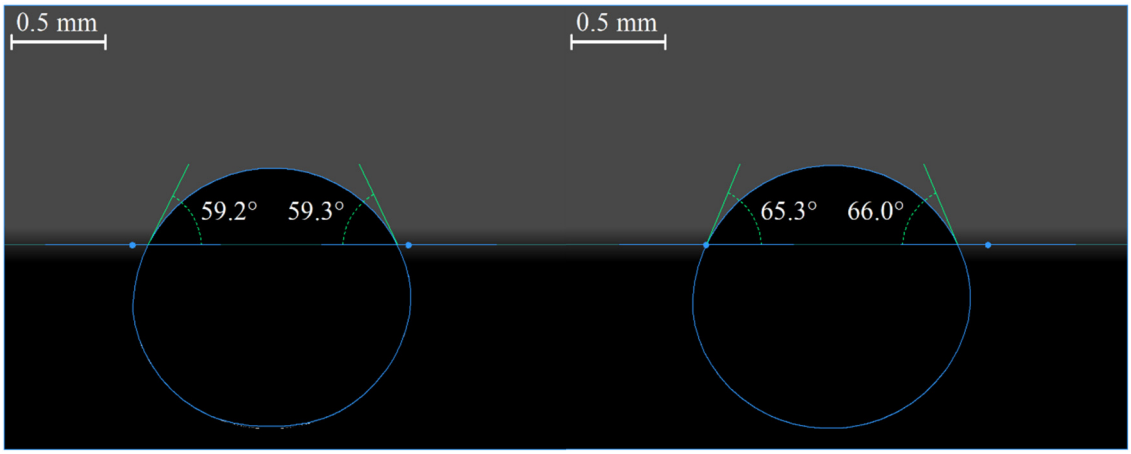

Fig. 3. Contact angle of the samples: ZrO_2–5wt.% CeO_2–10wt.% SiC (a) and Al_2O_3–20wt.% SiO_2–10wt.% ZrO_2 (b)

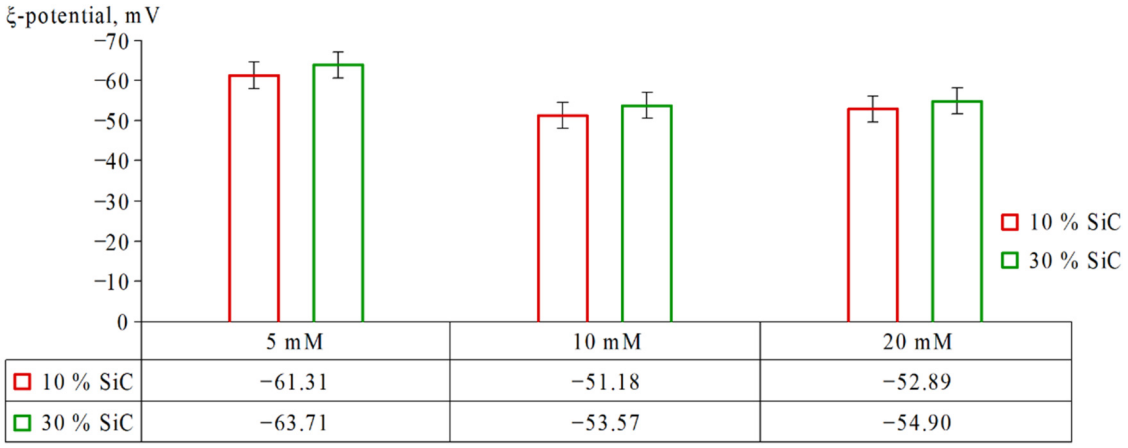

	5 mM	10 mM	20 mM
10 % SiC	−61.31	−51.18	−52.89
30 % SiC	−63.71	−53.57	−54.90

Fig. 4. Zeta potentials of ZrO_2–5wt.% CeO_2–10wt.% SiC and ZrO_2–5wt.% CeO_2–30wt.% SiC mixtures at concentrations of 5 mM,10 mM and 20 mM

surface. The surface of the composites is smooth and uniform with small pores (Fig. 2).

The contact angles of ZrO_2–5wt.% CeO_2–10wt.% SiC and Al_2O_3–20wt.% CeO_2–10wt.% ZrO_2 samples are given in Table 1.

To determine the electrostatic behavior of the starting powders, the zeta potentials of the particle suspension were measured. Suspensions were prepared by adding the appropriate mass of ZrO_2–5wt.% CeO_2–10wt.% SiC and ZrO_2–5wt.% CeO_2–30wt.% SiC mixtures to distilled water in order to obtain concentrations of 5 mM,10 mM and 20 mM. The results of zeta potential measurements indicate that the nanoparticles have negative charge in all the cases of the present study (Fig. 4).

MG-63 cells were cultured on discs with compositions of ZrO_2–5 wt.% CeO_2–10 wt.% SiC sintered at 1300°C, holding time 10 min, ZrO_2–5wt.% CeO_2 sintered at 1300°C, holding time 3 min, ZrO_2–5wt.% CeO_2 sintered at 1400°C, holding time 3 min, and Al_2O_3–20wt.% SiO_2–10wt.% ZrO_2, sintered at 1600°C, holding time 5min (Fig. 5).

The growth dynamics of MG-63 cells on the surface of zirconium, cerium, and aluminium ceramics samples was estimated during 24 days of cultivation by counting the number of nuclei per unit surface area. The samples showed no signs of cell death (Fig. 5a, 5b). Otherwise, it would be necessary to talk about disturbances in the adhesion of MG-63 cells to the substrate.

The surface properties of the investigated ceramic systems provide normal viability of the MG-63 culture, which indicates that ceramic systems are promising for the production of bone implants for orthopaedics.

Fig. 5c shows that the composite ceramics ZrO_2–5wt.% CeO_2–10wt.%SiC (sintered at 1300°C, holding time 10 min) has cell viability of 66%. The sample ZrO_2–5wt.% CeO_2 (sintered at 1300°C, holding time 3 min) represents 33%, meanwhile the sample ZrO_2–5wt.%CeO_2 (sintered at 1400°C, holding time 3 min) has 60%. Cell viability for the system Al_2O_3–20wt.% SiO_2–10wt.% ZrO_2 (sintered at 1600°C, holding time 5min) is 53%. The sintering mode at high temperature and holding time of up to 3 minutes affects the biocompatibility of ceramics.

Samples ZrO_2–5wt.% CeO_2 (sintered at 1400°C, holding time 3 min) and ZrO_2–5% CeO_2–10% SiC, (sintered at 1300°C, holding time 10 min) ensure the highest cell viability in the MG-63 cells.

With an increase in the proportion of additives, the mechanical characteristics of ceramic systems for biomedical structures improve; in particular, the Young's modulus decreases, which contributes to better cell adhesion. Varying the qualitative and quantitative composition of zirconia based composites and choosing the optimal sintering mode allows us to create a material that ensures the best interaction of the implant with cells and tissues. Consider-

Table 1. Contact angles of samples

Sample	CA(m), °	St.dev.
ZrO_2–5wt.% CeO_2–10wt.% SiC	58.00	1.92
Al_2O_3–20wt.% CeO_2–10wt.% ZrO_2	66.65	1.97

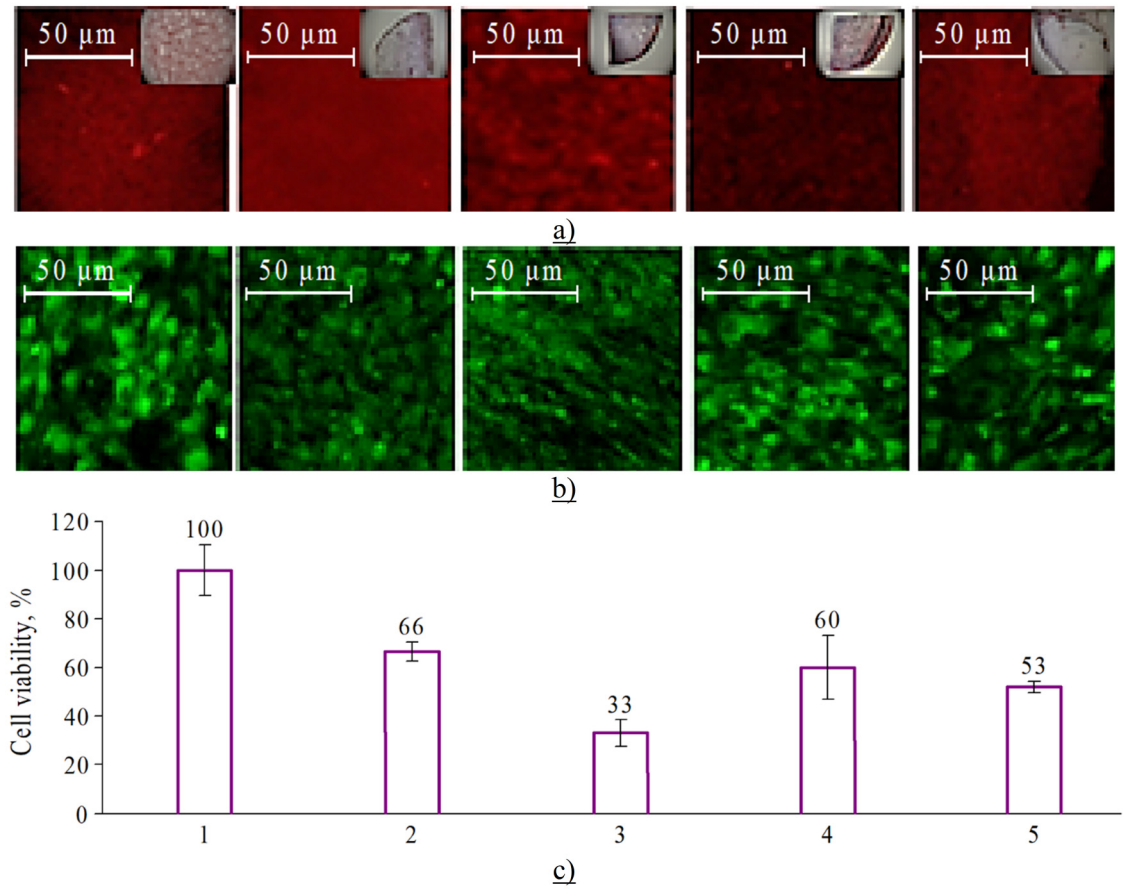

Fig. 5. Images of Leica stereomicroscope (pink) and a confocal Zeiss microscope (red) for Alizarin Red staining of calcium (a); the confocal Zeiss microscope images for Cell Tracker Red staining for cell density and morphology studies 24 days after seeding (b); MG-63 cells viability studies on the samples: polystirene (1), ZrO_2–5wt.% CeO_2–10wt.% SiC sintered at1300°C, holding time 10 min (2), ZrO_2–5wt.% CeO_2 sintered at 1300°C, holding time 3 min (3), ZrO_2–5wt.% CeO_2 sintered at 1400°C, holding time 3 min (4), Al_2O_3–20wt.% SiO_2–10wt.% ZrO_2, sintered at1600°C, holding time 5min (5) (c)

ing the excellent anticorrosion properties and biocompatibility, zirconia-based ceramics is promising for biomedical implants and devices. The surface properties and long-term performance of biomaterials, especially those used in surgical implants and medical devices, are mainly determined by surface modification techniques.

4. Conclusions

To conclude, the formation of ceramic systems of composition based on partially stabilized zirconia by hot pressing of nanopowders obtained by decomposition from fluoride salts, as well as the biocompatibility of the developed systems were studied. The analysis of cell viability showed, that ZrO_2–5wt.% CeO_2–10wt.% SiC ceramics has good biocompatibility with MG-63 cells. It has been established that the greatest biocompatibility is demonstrated by composites sintered in the temperature range of 1300–1600°C. These results indicate that the ZrO_2–5wt.% CeO_2–10wt.% SiC composite formed at 1300°C, as well as Al_2O_3–20% SiO_2–10% ZrO_2 sintered at 1600°C may be useful for improving the biocompatibility of MG-63 cells in vitro.

Acknowledgments

The article was prepared as part of a study under the state budget topic The Use of Non-traditional Methods of Obtaining Nanopowders and Sintering in the Development of Modified Mullite-ZrO_2 Ceramics Resistant to Heat Shock (State Registration Number 0121U109441) with the financial support of the Ministry of Education and Science of Ukraine. Grants PID2021-127191OB-I00, and RYC2018-025502-I funded by MCIN/AEI/10.13039/501100011033, "ERDF A way of making Europe" and "ESF Investing in your future".

References

1. E.L.Pang, G.B.Olson, C.A.Schuh, *Acta Materialia*, **213**, 116972 (2021). doi: https://doi.org/10.1016/j.actamat.2021.116972.
2. N.Knoblauch, P.A.Mechnich, *Crystals (Basel)*, **11(8)**, 885 **(**2021). doi: https://doi.org/10.3390/cryst11080885.
3. R.C.O'Brien, R.M.Ambrosi, N.P.Bannister, et al., *Journal of Nuclear Materials*, **393**, 108 (2009). doi: https://doi.org/10.1016/j.jnucmat.2009.05.012.
4. R.Bacani, T.S.Martins, M.C.Fantini, D.G.Lamas, *Journal of Alloys and Compounds*, **671**, 396 (2016). doi: https://doi.org/10.1016/j.jallcom.2016.01.213.
5. Z.Krzysiak, E.Gevorkyan, V.Nerubatskyi, M.Rucki, V.Chyshkala, J.Caban, T.Mazur, *Materials*, **15(17)**, 6073 (2022). doi: https://doi.org/10.3390/ma15176073.
6. L.Lan. S.Chen, Y.Sao, M.Gong, Y.Chen, *Catalysis Science&Techology*, **5(9)**, 4488 (2015). doi: https://doi.org/10.1039/C5CY00612K.
7. T.Jiang, S.Yuchang, H.Te, Y.Qiushan, T.Rabigul, L.Quan, X.Yunze, *Solid State Ionics*, **292**, 22 (2016). doi: https://doi.org/10.1016/j.ssi.2016.03.018.
8. O.Y.Kurapova, S.M.Shugurov, E.A.Vasil'eva, D.A.Savelev, V.G.Konakov, S.I.Lopatin, *Ceramics International*, **8(47)**, 11072 (2021). https://doi.org/10.1016/j.ceramint.2020.12.230.
9. Y.Dong, Z.Liu, L.Pang, Y.Han, S.Yao, X.Wang, *Physica B: Condensed Matter*, **612** (2021). doi: https://doi.org/10.1016/j.physb.2021.412972.
10. B.Dou, D.Yang, T.Kang, Y.Xu, Q.Hao, F.Bin, X.Xu, *Carbon Resources Conversion*, **4**, 55 (2021). doi: https://doi.org/10.1016/j.crcon.2021.01.007.
11. J.Wang, J.Sun, Q.Jing, B.Liu, H.Zhang, Y.Yongsheng, et al,. *Journal of the European Ceramic Society*, **38(7)**, 2841 (2018). doi: https://doi.org/10.1016/j.jeurceramsoc.2018.02.019.
12. O.Y.Kurapova, S.N.Golubev, A.G.Glukharev, V.G.Konakov, *Refractories and Industrial Ceramics*, **61(1)**, 112 (2020). doi: https://doi.org/10.1007/s11148-020-00440-0.
13. J.Arfaoui, A.Ghorbel, C.Petitto, G.Delahay, *Journal of Industrial and Engineering Chemistry*, **95**, 182 (2021). doi: https://doi.org/10.1016/j.jiec.2020.12.021.
14. T.K.Phung, L.P.Hernández, G.Busca, *Applied Catalysis A: General*, **489**, 180 (2015). doi: https://doi.org/10.1016/j.apcata.2014.10.025.
15. E.Gevorkyan, V.Nerubatskyi, V.Chyshkala, O.Morozova, *Eastern-European Journal of Enterprise Technologies***, 5(12(113)), 6 (2021).** doi: https://doi.org/10.15587/1729-4061.2021.242503.
16. E.Gevorkyan, V.Nerubatskyi, V.Chyshkala, Y.Gutsalenko, O.Morozova, *Eastern-European Journal of Enterprise Technologies***, 6(12(114)), 40 (2021).** doi: https://doi.org/10.15587/1729-4061.2021.245938.
17. M.Tokita, *Ceramics*, **4**, 160 (2021). doi: https://doi.org/10.3390/ceramics4020014.
18. E.S.Gevorkyan, D.S.Sofronov, V.P.Nerubatskyi, V.O.Chyshkala, O.M.Morozova, O.M.Lebedynskyi, P.V.Mateychenko, *Journal of Superhard Materials*, **45(1)**, 31 (2023). doi: https://doi.org/10.3103/S1063457623010057.
19. T.Tite, A.C.Popa, L.Balescu, I.Bogdan, I.Pasuk, J.Ferreira, G.Stan, *Materials*, **11(11)** (2018). doi: https://doi.org/10.3390/ma11112081.
20. Y.Al-Mahdy, H.Eltayeb, , *Al-Azhar Journal of Dentistry,* **5:1 (11)**, 89 (2018). doi: https://doi.org/10.21608/adjg.2018.7996.
21. K.N.Ho, L.W.Chen, T.F.Kuo, K.S.Chen, S.Y.Lee, S.F.Wang, *Journal of Dental Sciences*, **18(1)**, 73 (2023). doi: https://doi.org/10.1016/j.jds.2022.06.007.
22. E.S.Gevorkyan, V.P.Nerubatskyi, R.V.Vovk, V.O.Chyshkala, M.V.Kislitsa, *Journal of Superhard Materials*, **44(5)**, 339 (2022). doi: https://doi.org/10.3103/S1063457622050033.
23. V.P.Nerubatskyi, R.V.Vovk, M.Gzik-Szumiata, E.S.Gevorkyan, *Low Temperature Physics,* **49(4)**, 540 (2023). doi: https://doi.org/10.1063/10.0017596.